Short-Range Ordering and the Abnormal Mechanical Properties of a Ni–20% Cr Alloy

N. R. Dudova[a], R. O. Kaibyshev[a], and V. A. Valitov[b]

[a]*Belgorod State University, ul. Pobedy 85, Belgorod, 308015 Russia*

[b]*Institute for Metals Superplasticity Problems, Russian Academy of Science, ul. St. Khalturina 39, Ufa, 450001 Russia*

Abstract—Effect of temperature on mechanical properties of a Ni–20% Cr alloy with an initial grain size of 100 μm in the temperature interval 150–1000°C (0.25–0.8 T_m) has been studied. It is shown that in the temperature range 400–600°C the alloy demonstrates a positive temperature dependence of both the flow stress and the coefficient of strain hardening and exhibits Portevin–le Chatelier effect (PLC). It has been established on the basis of a comparison of data of calorimetric studies and temperature dependence of mechanical properties that the unusual mechanical behavior of Ni–20% Cr alloy is a result of the occurrence of short-range order. The nature of the effect of the short-range order on the mechanical properties is discussed.

Key words: Ni–20% Cr alloy, short-range ordering, mechanical properties

INTRODUCTION

As is known, the short-range ordering in the arrangement of atoms of different type in crystalline alloys consists in their mutually ordered arrangement at distances slightly higher than interatomic and is independent of orientation [1]. A short-range order appears in solid solutions in specific temperature ranges and leads to a substantial change in the physical and mechanical properties of materials [1]. This phenomenon has great practical value for the superalloys, since it makes it possible to increase their resistance to creep [2]. At present, of greatest practical application are superalloys on the basis of the Ni–Cr system [3]. They are the most common materials for the operation at temperatures higher than 650°C. Sims et al. [3] analyzed five mechanisms of strengthening of superalloys in detail. However, no effect of short-range ordering in the solid solution of the Ni–Cr system on the strength characteristics of superalloys was examined despite the fact that it leads to an increase in the strength of these alloys with increasing temperature [4–6].

In the alloy Kh20N80 (Ni–20% Cr) there was observed a well-known *K*-state effect—an increase in the electrical resistance in the range of temperatures of 400–550°C with increasing temperature [6–8]. This phenomenon is explained by the formation of a short-range ordering in the samples of Ni–20% Cr quenched in water from high temperatures [6]. It should be noted that in the temperature range of the short-range ordering (400–550°C) t an abnormal increase takes place in both the electrical resistance and strength characteristics of nichrome [4–12]. This makes it possible to assume that it is the short-range order that is the reason for an increase in hardness and stresses of plastic flow with increasing temperature in this interval [4, 6, 10], as well as an increase in the creep resistance [9, 13]. These phenomena, which are uncommon for metals, are called the "positive temperature dependence of the flow stresses" (an increase in the flow stresses with increasing temperature) [14–16], and the "negative creep" (a compression of samples in the process of tensile tests for creep) [9].

In Ni–Cr alloys, an ordering leads to the formation of a phase with an Ni_2Cr superstructure (Pt_2Mo type) [6, 11, 17–19]. This ordering can be both short-range and long-range type. A long-range order, as a rule, occurs in Ni–Cr–*X* alloys with a stoichiometric composition, and the predominantly short-range order is observed in the alloys with a nonstoichiometric composition, such as, for example, Ni–20% Cr [6–8, 11]. An increase in the content of Cr, additives of Mo, and also an increase in the holding time in the range of temperatures 400–650°C lead to the formation of long-range-order domains in the matrix with a short-range order. The phase with a long-range order is observed in Ni–Cr alloys with a content of chromium more than 25% or with additions of elements that replace Cr in the Ni_2Cr phase [11, 17–19]. Especially effective for the formation of the superstructure with an orthorhombic lattice are the additives of Mo [11, 19]. An ordered Ni_2Cr domain has a size of 4 nm or less and is connected with the γ matrix by coherent boundaries [19]. It should be noted that the formation of second phases with a super-

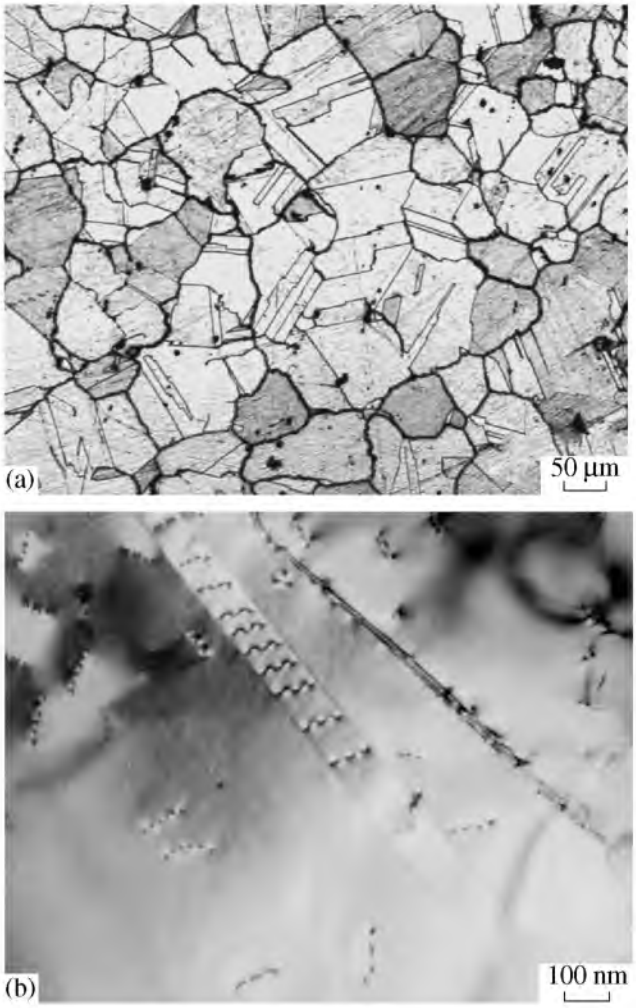

Fig. 1. Initial coarse-grained microstructure of Ni–20% Cr alloy: (a) optical micrograph and (b) electron micrograph (TEM).

structure radically changes the electrical conductivity and sharply decreases the plasticity [11, 17–19]. A long-range ordering with the formation of an $Ni_2(Cr,Mo)$ phase is undesirable for the superalloys since leads to their embrittlement [11, 17–19]. At the same time, the short-range order in Ni–20% alloy can be the main reason for the high creep strength of this material at temperatures near 600°C.

Nichrome and the superalloy Nimonic 80 designed on its basis were the first industrial nickel-base superalloys. However, even after 65 years of their industrial use the physical mechanisms which ensure their high mechanical properties remain insufficiently clear. This work is devoted to the consideration of the effect of short-range ordering on the mechanical properties of a Ni–20% alloy with such a small (0.05%) carbon content, that excludes its significant influence on the processes occuring upon heating.

EXPERIMENTAL

The Kh20N80 alloy used in this work has the following chemical composition: Ni (base)–21% Cr–1.1% Si–0.6% Mn–0.75% Fe–0.31% Al–0.08% Ti–0.35% Cu–0.05% C. A homogeneous structure with an average grain size of 100 μm was produced by annealing a hot-rolled bar with a diameter of 40 mm at $T = 1025$°C for 2 h with a subsequent cooling in air. The mechanical compressive tests of cylindrical samples with dimensions of ∅10 × 12 mm were performed on a Schenck universal dynamometer in a temperature range 150–1000°C at an initial strain rate 7×10^{-4} s^{-1}. The procedures of mechanical tests and microstructural characterization were described in detail in Ref. [10].

The coefficient of strain hardening was determined by the equation [20]

$$\theta = 1/4(d\sigma/de), \quad (1)$$

where σ is the true applied stress, and e is the true strain.

The electron-microscopic examinations of thin foils were performed using a JEM-2000 EX transmission electron microscope (TEM) at an accelerating voltage of 160 kV and a JEM-2100 electron microscope at an accelerating voltage of 200 kV. The foils were obtained by the method of jet polishing using an electrolyte consisting of a 10% solution of perchloric acid in *n*-butanol. The dislocation density was calculated as the density of etch pits on the foil surface [21].

The calorimetric studies (DSC) were performed using an SDT Q600 device (TA Instruments). The samples had the form of disks with a weight changing from 30 to 90 mg. The measurements were carried out upon heating of samples at a rate of 2, 10, and 20 K/min.

RESULTS

Initial Microstructure

The initial coarse-grained structure ($d = 100$ μm) is characterized by the presence of a high fraction (50%) of twin boundaries (Fig. 1a). The dislocation density is small (does not exceed 2×10^{13} m^{-2} (Fig. 1b)).

Thermal Analysis

Figure 2a shows three calorimetric curves. The first curve shows the calorimetric data for a sample that was quenched in water from a temperature of 1050°C after holding for 20 min and then heated at a rate of 20 K/min. In this curve, there is well seen an exothermic peak at a temperature of 388°C, which is ascribed to the formation of particles of a second phase [11, 22, 23]. The second weak exothermic peak is observed at a temperature of 546°C. These two peaks can be interpreted as a result of short-range ordering [11].

At $t = 388$°C, the short-range order can occur as a result of migration of Cr atoms due to their interaction with quenching-induced vacancies of a high density

[11]. It was shown in [5] that the density of quenched vacancies has a significant effect on the kinetics of short-range ordering; the higher the density of vacancies, the higher the increase in the electrical resistance as a result of short-range ordering. At the same time, it was shown in [24] that the vacancies that are excessive in comparison with their equilibrium concentration are annihilated at various sinks before a short-range ordering starts to occur. This made it possible to assume that this peak can be connected with the precipitation of carbides. However, the electron-microscopic studies revealed carbides of the $M_{23}C_6$ type (Fig. 2b) in the alloy already after quenching from 1050°C, i.e., before the DSC study. They have an elongated shape with a width that varies from 0.2 to 1 μm and a length from 0.5 to 2 μm. An estimation of their volume concentration (~0.5%) showed that the entire carbon present in Ni–20% Cr alloy must enter into the composition of these carbides. Accordingly, the volume concentration and the size of carbides after aging of the quenched sample for 30 min at 540°C did not change. This indicates that the heating to 540°C does not lead to an additional precipitation of carbides, and the both clearly pronounced exothermic peaks at 388 and 546°C cannot be attributed the precipitation or dissolution of carbides, so that the assumption of the authors of [11] on the origin of the peak at 388°C with the occurrence of short-range order seems to be substantiated.

At T = 546°C, there occurs an additional ordering due to the self-diffusion of Cr atoms [11]. A further increase in temperature increases the diffusion rate to such an extent that there takes place a disordering [11]. A clearly pronounced endothermic peak, which usually is ascribed to the dissolution of second phases [22], is observed at a temperature of 599°C. Correspondingly, this endothermic peak can be interpreted as a result of disordering.

The second curve in Fig. 2a was obtained using the same sample but heated at a rate of 2 K/min. In this curve, the first exothermic peak is displaced almost by 100 K toward higher temperatures. The second exothermic and the endothermic peaks are located at almost the same temperatures as in the sample heated at a rate of 20 K/min. At temperatures of ~879 and ~970°C, there are observed endothermic peaks that were not revealed upon heating at a rate of 20 K/min. They can be associated with the dissolution of carbides during heating at a slow rate [11].

The third curve in Fig. 2a was obtained at a heating rate of 10 K/min for the sample cooled with a furnace after annealing at T = 1050°C. The curve has weakly pronounced exothermic peaks at a temperature ~390°C and an endothermic peak at a temperature ~563°C. A small endothermic peak takes place at 674°C. In all likelihood, the disordering in the sample cooled with a furnace terminates at this temperature, which is higher than that for the quenched samples. The slowly cooled material upon reheating is already in an ordered state.

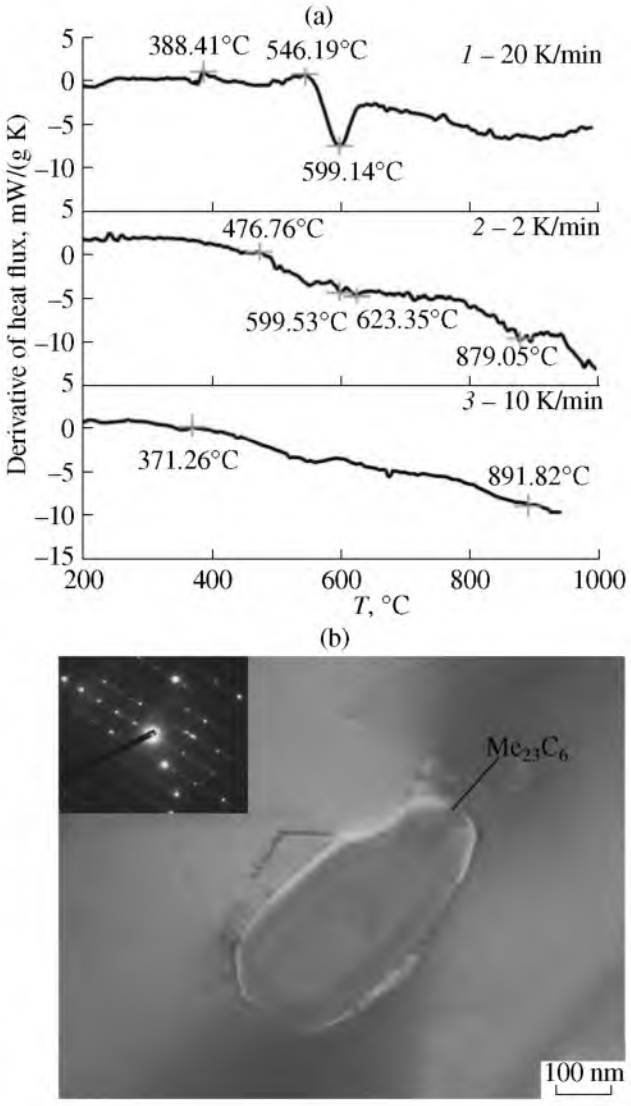

Fig. 2. (a) Calorimetric curves taken during heating of Ni–20% Cr alloy (curves *1–3* are described in the main text). (b) Fine microstructure of Ni–20% Cr alloy after quenching from 1050°C.

This can lead to a larger size of the regions of short-range ordering in comparison with the quenched material and thereby specify an elevated temperature of disordering. Only a weak temperature influence on the thermal effects can also be obserwed because of an insignificant extent of additional short-range ordering. Note that the data of thermal analysis correlate well with the data on the temperature dependence of electrical resistance reported in [7, 8, 11, 12]. The sample cooled with a furnace demonstrates only weak signs of ordering both upon the thermal analysis and in measurements of the temperature dependence of electrical resistance [11].

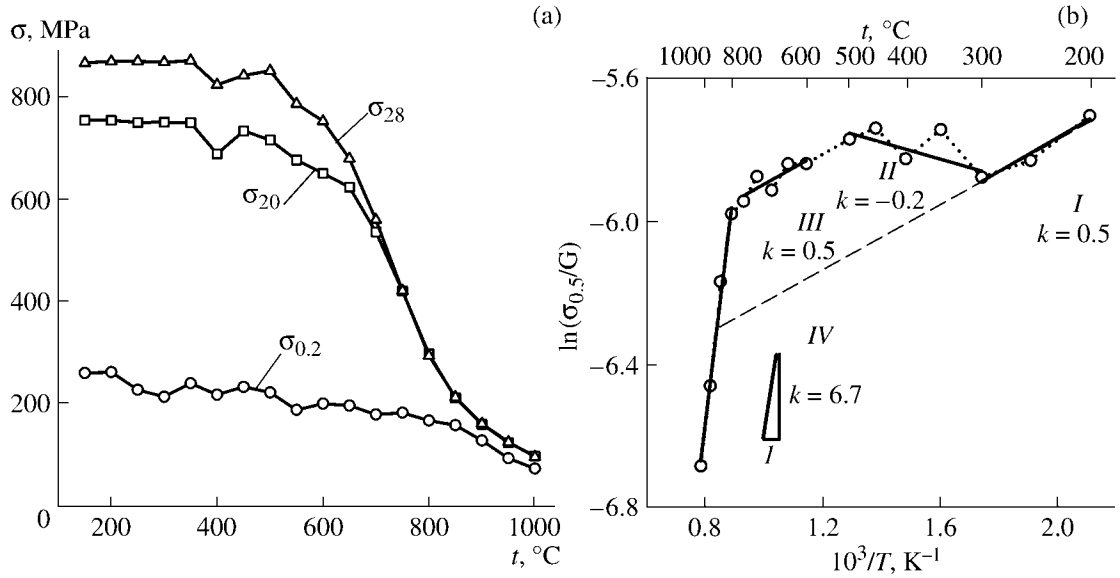

Fig. 3. (a) Temperature dependence of the yield stress$\sigma_{0.2}$ and flow stresses σ_{20} and σ_{28}; and (b) semilogarithmic plate dependence of the yield stress $\sigma_{0.2}$ normalized to the temperature dependence of the shear modulus $G(T)$ on the reciprocal temperature.

Mechanical Properties

Figure 3a displays the temperature dependences of the yield stress $\sigma_{0.2}$ and flow stresses that correspond to the degree of deformation of 20 and 28% at a strain rate $\varepsilon = 7 \times 10^{-4}$ s^{-1}. The yield stress decreases with increasing temperature in the range of 200–300°C, and the flow stresses σ_{20} and σ_{28} change weakly up to 350°C. With a further increase in temperature, an increase in $\sigma_{0.2}$ takes place; in the temperature dependence of the stresses σ_{20} and σ_{28} there takes place a minimum at 400°C, after which they also increase. The increment in the yield stress at 450°C in comparison with its value at 300°C is 10%. The increase in the values of σ_{20} at $t = 450$°C and of σ_{28} at $t = 500$°C in comparison with their values at 400°C does not exceed 7%. It can be concluded that in the temperature range of 300–500°C we have a positive temperature dependence of the flow stress without a clearly pronounced peak.

As the temperature increases to above 500°C, the magnitudes of $\sigma_{0.2}$, σ_{20}, and σ_{28} begin decreasing (Fig. 3a). However, the rate of their decrease is different. The values of the flow stresses σ_{20} and σ_{28} decrease very rapidly, and the yield stress decreases slowly. At 700°C, the values of σ_{20} and σ_{28} become comparable; at $t \geq 850$°C, the values of the yield stress and the flow stresses at high degrees of deformation become almost the same; the plastic flow attains the steady-state almost immediately after the onset of plastic deformation. The rate of the decrease in σ_{20} and σ_{28} with increasing temperature in the interval of 500–650°C is slightly greater than that at $t < 350$°C, and with a further increase in the temperature to above 650°C the flow stress decreases quite rapidly (Fig. 3a). Thus, in the case of flow stresses at relatively large degrees of deformation (20–30%) the abnormal mechanical behavior manifests itself only in the appearance of a positive temperature dependence in the interval 400–500°C. The yield stress demonstrates both a positive temperature dependence and a slowing-down effect of the rates of decrease in stresses ("after-effect") in the range of temperatures of 600–850°C.

In the graph of the variation of the yield stress normalized to the shear modulus $G(T)$ as a function of the reciprocal temperature plotted in semilogarithmic scales, it is possible to distinguish four temperature ranges (Fig. 3b) differing in the rate of the decrease in the yield stress with increasing temperature. The first (200–300°C) and the third (600–800°C) temperature intervals are characterized by the same values of the coefficient $k = 0.5$, which can indicate the similar mechanisms of plastic deformation at these temperatures [21, 25]. The coefficient k, which is equal to the slope of the straight line $\ln(\sigma_{0.2}/G) - 1/T$, characterizes the rate of the decrease in the flow stress with increasing temperature and is used in calculations of the energy of activation [21, 25]. In the second temperature range (300–500°C) there is observed an increase in the normalized yield stress $\sigma_{0.2}/G$ with an increase in the temperature from 300 to 350°C and from 400 to 450°C. In spite of the large spread of experimental points because of the Portevin–Le Chatelier effect, it can be assumed that in the range of 300–500°C there is observed a tendency of an increase in $\sigma_{0.2}/G$ with increasing temperature. In this case, the coefficient k takes negative value (–0.2). It should be noted that in metals the positive temperature dependence of flow stresses is observed extremely rarely [15]. In the fourth temperature range, at $t \geq 800$°C, there is observed a rapid fall off of the normalized flow stresses (k = 6.7). Thus, an analysis of Fig. 3b shows that the yield stress decreases with

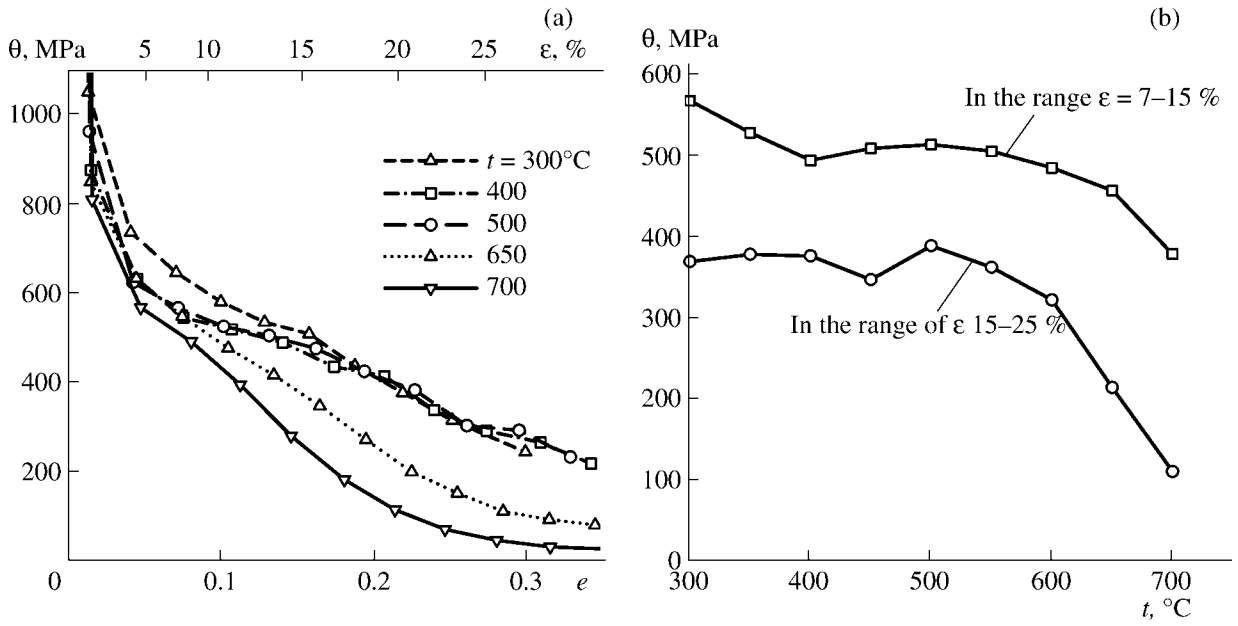

Fig. 4. Variation of the coefficient of strain hardening θ depending on (a) the strain and (b) the temperature of deformation.

increasing temperature in the entire temperature interval except for 400–500°C, where there is observed an anomaly of plastic flow, as in [4, 6].

In order to examine the nature of the phenomenon of "aftereffect," we plotted temperature dependences of the coefficient of strain hardening θ (Fig. 4). It is seen that the strain and the temperature of deformation strongly influence strain hardening. It is possible to roveal two regions of strains, which are distinguished by the rate of the decrease in the coefficient of strain hardening (Fig. 4a). At small strains, there is observed a rapid decrease in the coefficient θ. At the strains larger than 5%, the rate of the drop in the coefficient of strain hardening is considerably less and it virtually does not change up to values close to zero. The rate of the decrease in the coefficient θ with increasing strain is maximum at $T \geq 650$°C and is minimum at 400–500°C. At the strain greater than 30%, the coefficient θ in this temperature interval becomes greater than that at 300°C. This explains the fact of the absence of "aftereffect" for the flow stresses at the strains of 20 and 28% at temperatures higher than 600°C (Fig. 3a). Note that the strains at which there occurs a transition from the stage of the rapid decrease of the coefficient θ to the stage of its slow decrease are close to the critical strains ε_{cr} at which serrations appear in the σ-*e* curves (PLC effect) [10].

The examination of the effect of temperature on the coefficient θ (Fig. 4b) shows that the strain hardening decreases with increasing temperature at $t < 400$°C. In the temperature range of 400–600°C, there is observed a maximum of the coefficient θ (it is possible to speak of the appearance of a positive temperature dependence of strain hardening). At $t \geq 650$°C, the coefficient θ decreases rapidly.

A specific feature of the mechanical behavior of coarse-grained Ni–20% Cr alloy in the temperature range of 300–600°C, which includes the temperatures of the appearance of short-range order, is the discontinuous flow (DF), when in the σ-*e* curves there appears a characteristic serration (Fig. 5). Note that each stress drop is accompanied by acoustic emission. A detailed analysis of this phenomenon is given in our previous work [10]. In this work, we will examine only the temperature effect on the shape of the σ-*e* curves at a constant strain rate (Fig. 5). With an increase in the deformation temperature, there is observed a change in the nature of serration in the σ-*e* curves. Below $t = 150$°C, there are observed smooth stress–strain curves (curve *1* in Fig. 5a). At $t = 250$–500°C, oscillations of flow stresses appear in the σ-*e* curves (curves *2* and *3* in Fig. 5a). There appear saw-tooth serrations with a change in the flow stresses of approximately 1–5% relative to the applied stresses. The height of the teeth in the curves has a clearly pronounced tendency to growth with an increase in the strain and temperature of deformation. At $t = 550$–600°C, teeth with a wide plateau (curves *4* and *5* in Fig. 5b) appear in the σ-e curves. Their relative height can reach 10% of the applied stresses at the strains of 30% or more. With an increase in the temperature to above 650°C, the σ-*e* curves again become smooth (curve *6* in Fig. 5b).

Microstructural Changes

Figure 6 displays the evolution of the fine structure upon deformation at a temperature of 500°C. Already

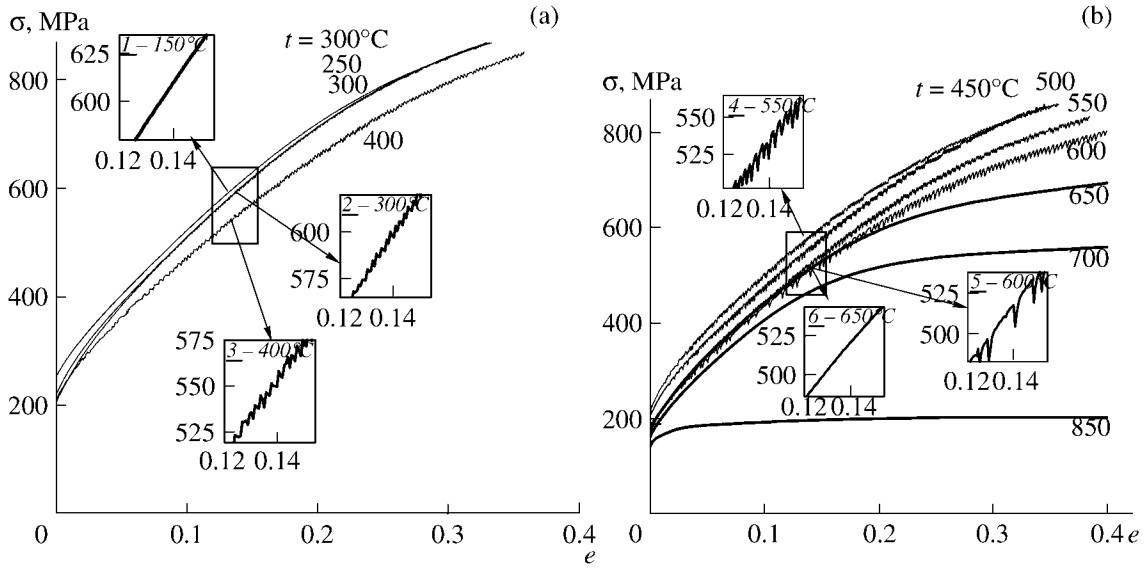

Fig. 5. True flow-stress– true-strain curves of Ni–20% Cr alloy. Curves *1–6* are described in the main text.

after deformation to ε = 3%, there is observed a dislocation emission from sources of the of Frank–Read type [10, Fig. 4a]. Planar dislocation pileups are formed. After ε = 10% (Fig. 6a), the dislocation density in the planar pileups increases considerably (Fig. 7). Some dislocations leave the planar pileups. At the leading dislocations of the planar pileups and at some other dislocations, the precipitation of particles of second phases is observed (the distance between the precipitates is 15–20 nm). A characteristic bowing of dislocation lines between these particles under the action of the applied stresses is seen [25–27]. However, this bowing and, therefore, the force of interaction between the precipitated particles and the moving dislocations [26] is substantially less than for the particles which cannot be cut by the dislocations [25–27] despite the fact that the applied stresses were high (approximately 500 MPa).

Deformation to ε = 30% leads to the formation of a cellular structure (Fig. 6b). The dislocation density increases by an order of magnitude (Fig. 7). Twisted dislocation lines form boundaries of irregular shape. This structure is characterized by high internal stresses due to dislocation pileups. At dislocations, particles with a size of 1.5–3 nm are observed, whose diffraction contrast indicates the coherent nature of their phase boundaries. Note that the dislocations at which particles of relatively large size, in comparison with those observed at ε = 10%, are located in the majority of cases are not bent under the action of the applied stresses.

After the strain reaches 50%, the dislocation density rises so (Fig. 7) that the separate dislocations become hardly resolvable (Fig. 6c). Moiré patterns are observed, whose appearance is connected with the arrangement of several layers of dislocations over the thickness of the foil. The size of arising dislocation cells decreases with increasing strain. Microscopic deformation bands appear. Thus, at ε = 50% there is formed a well-defined low-energy dislocation structure (LEDS) [28]. A very small quantity of particles is observed with a size of no more than 4 nm. Their volume concentration is less than 1%. As the strain increases to ε = 70% (Fig. 6d), a LEDS forms that is typical of the cold-deformable metals with an fcc lattice. Macrobands are formed, which are divided into separate regions by microbands and dense dislocation walls (DDWs) [28]. The nature of the Moiré patterns indicates an increase in the density of lattice dislocations in comparison with that observed at ε = 50% (Fig. 7).

DISCUSSION

The experimental results obtained in this work indicate that the abnormal mechanical properties of Ni–20% Cr alloy are connected with the formation of a short-range-order structure, which agrees well with the data of works [4, 10–12]. The positive temperature dependence of the flow stresses and of the coefficient of strain hardening θ, as well as the PLC effect [10], are observed in the temperature interval of 400–600°C, which, according to the calorimetric data, coincides with the temperature interval in which short-range ordering occurs. The short-range order not only increases the yield stress of Ni–20% Cr alloy at $t \le 600$°C, but also ensures a higher level of the strength properties in the interval of 600–750°C. In Fig. 3b, it is well seen that straight line III lies considerably higher than straight line I extrapolated into the temperature range of 600–800°C. The distance between these two straight lines is a quantitative characteristic of the phenomenon of "aftereffect" caused by short-range order, which ensures an increase in the working temperature of Ni–20% Cr alloy in comparison with

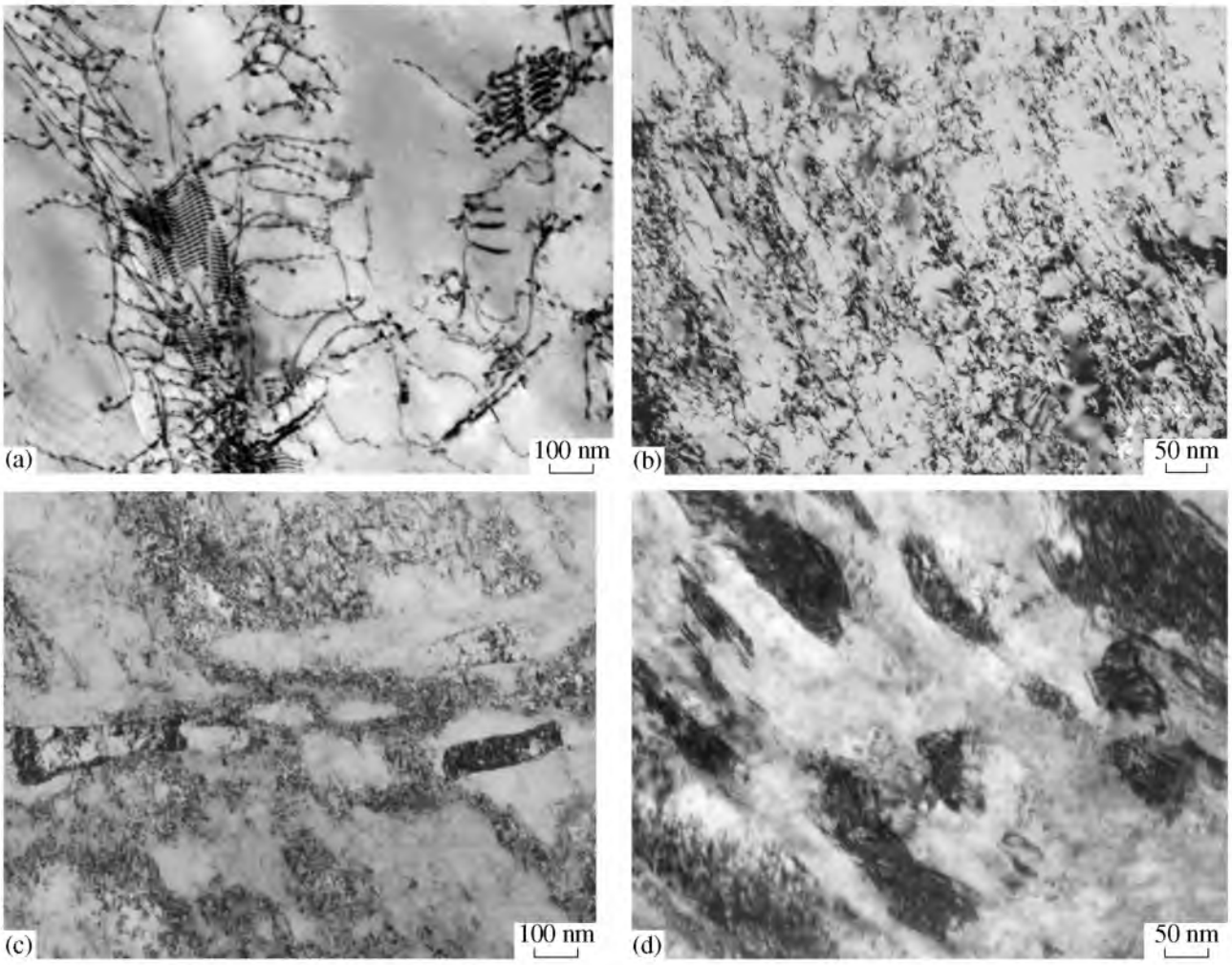

Fig. 6. Evolution of the fine structure of Ni–20% Cr alloy after deformation at $T = 500°C$ at a strain rate of 7×10^{-4} s^{-1}: (a) $\varepsilon = 10\%$, (b) 30%, (c) 50%, and (d) 70%.

homogeneous high-temperature steels and alloys in which no short-range order exists.

Note that the minimum of the yield stress $\sigma_{0.2}$ observed (Fig. 3a) at 300°C is small (about 10%). This "dip" in the yield stress, whose value is used for calculating parts exploited at high temperatures (to 650–750°C), is of no large practical sense.

The short-range order exerts a greatest effect on the value of strain hardening and, as a result, on the flow stresses at the strains higher than 20%. Because of the development of short-range ordering, the mobile dislocations are forced to cut clusters of Cr atoms, which requires enhanced stresses. This leads to an increase in $\sigma_{0.2}$ in the interval of 400–500°C with an increase in temperature. For this reason, single dislocations cannot move in the matrix with a short-range order because of the high stresses of internal friction in the lattice. The dislocation motion becomes a cooperative process [29]. The ability of moving is preserved only for dislocations located in planar pileups, since there occurs an increase in the effective stresses acting on the leading dislocations because of the superposition of the applied stresses and stresses that appear at the leading dislocation of the planar pileup. In the course of their cooperative movement, the dislocations of a planar pileup destroy short-range order, which leads to a decrease in the stresses of the resistance of lattice for moving dislocations. In the σ-e curves, a fall-off of stresses takes place [10] and a PLC effect is observed. The moving planar dislocation pileups can be blocked due to the formation, at the leading dislocations, of long-range-order domains with coherent boundaries, i.e. due to the development of long-range order caused by plastic deformation. The spacing between the long-range-ordered domains formed at the leading dislocations is very small, and therefore the precipitation strengthening is has a hihg value. For the leading dislocations to cut planar pileups of these dispersed particles, there are required enhanced stresses, which leads to an increase in the stresses in the σ-e curves. Since a particle with a superstructure should be cut by all moving dislocations

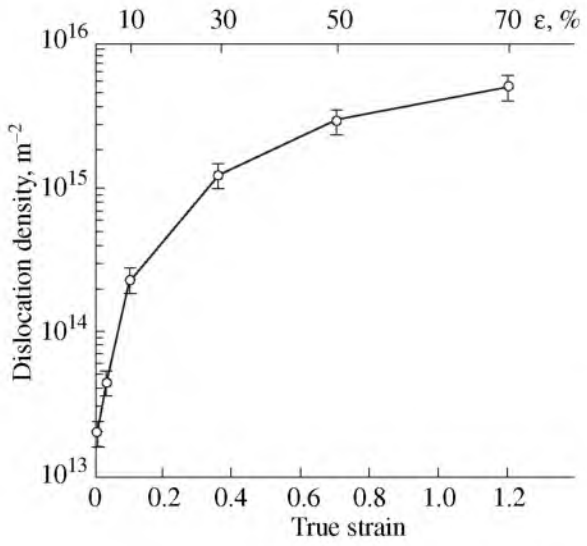

Fig. 7. Dislocation density as a function of the strain at T = 500°C.

of a given planar pileup, this leads to its "splitting", the size of the domain of long-range order can prove to become less than critical, and it become spontaneously dissolved. The unlocking of a planar pileup leads to a weakening of the material.

With increasing temperature, there occurs an increase in both the size of the dispersed particles precipitating at the leading dislocations and, in all likelihood, the size of regions of short-range order. To cut them, there are required ever greater stresses, and for "splitting" the long-range-ordered domains, the passage of ever larger number of dislocations is necessary. This leads to an increase in the amplitude of the oscillations of stresses and a decrease in their frequency. Therefore, the height and shape of serrations in the σ-e curves change with increasing temperature [10]. The presence of plateaus on the serrations indicates that a large number of dislocations passes through the regions of short-range ordering or the domains of long-range order before they dissolve. In all likelihood, an increase in the size of the fields of short-range order increases the mean free path of dislocations, which decreases the number of new dislocations generated by sources for continuing deformation. This leads to a decrease in the coefficient of strain hardening θ with an increase in the temperature to above 500°C. At $t > 600$°C, the short-range order no longer affects the accumulation of dislocations. There occurs a sharp decrease in the coefficient of strain hardening θ with an increase in the strain.

Thus, short-range ordering causes a heterogeneous nature of slip [10]. The consequences are the PLC phenomenon and an intense accumulation of lattice dislocations in the graininteriors. The latter is connected with the fact that the blocking of the motion of the absolute majority of mobile dislocations and a significant decrease in the length of their mean free path lead to the need for ensuring continuous plastic deformation due to a continuous generation of new dislocations at the existing sources for maintaining a necessary density of mobile dislocations. This leads to a strong increase in the total dislocation density (see Fig. 7), since there are required new and new dislocations for continuing plastic deformation. Thus, the existence of a short-range order provides a high rate of the accumulation of lattice defects and, correspondingly, increased magnitudes of the coefficient θ in comparison with the deformation at temperatures that are lower than the temperatures of short-range ordering.

The character of the evolution of the dislocation structure in the temperature range of short-range order is precisely the same as upon cold deformation [28]. At small strains, there occurs a sharp increase in the dislocation density, which specifies the high values of the coefficient θ. With increasing strains, there is activated a multiple slip [10], and processes of dislocation redistribution develop, leading to the formation of a LEDS [28], which is accompanied by the decrease in the degree of strain hardening. There is a correlation between the increase in the dislocation density ρ (see Fig. 7) and the effect of the strains on the coefficient of strain hardening θ (Fig. 4a).

Thus, an analysis of the variation of the mechanical properties of Ni–20% Cr alloy indicates that in this alloy there is formed a short-range-order structure at temperatures of 400–600°C. This specifies a positive temperature dependence of its strength characteristics and makes it possible to observe the Portevin–le Chatelier effect in it [10].

CONCLUSIONS

(1) Based on the data of thermal analysis, it has been established that upon heating of quenched Ni–20% Cr alloy the short-range ordering occurs at a temperature of 388°C. At a temperature of 599°C, the disordering occurs.

(2) In the temperature range of 400–500°C, Ni–20% Cr alloy demonstrates positive temperature dependences of the yield stress and of flow stresses at the strains equal to 20 and 28%. Furthermore, at these temperatures there is observed a positive temperature dependence of the coefficient of strain hardening θ at the strains exceeding 20%.

(3) The Portevin–le Chatelier effect in Ni–20% Cr alloy is caused by short-range ordering.

(4) The evolution of the dislocation structure in the process of the plastic deformation of Ni–20% Cr alloy in the temperature range of short-range ordering is analogous to the evolution of structure in fcc metals at room temperature. The formation of low-energy dislocation structures leads to a decrease in the degree of strain hardening with an increase in the strain.

ACKNOWLEDGMENTS

The authors are grateful to the Joint Research Center, Belgorod State University and personally to Dr. I. Tarasova for assistance with thermal analysis.

REFERENCES

1. V. I. Iveronova and A. A. Katsnel'son, *Short-Range Order in Solid Solutions* (Nauka, Moscow, 1977) [in Russian].
2. B. E. Panin, E. F. Dudarev, and L. S. Bushnev, *Structure and Mechanical Properties of Substitutional Solid Solutions* (Metallurgiya, Moscow, 1971) [in Russian].
3. Ch. T. Sims, N. S. Stoloff, and W. C. Hagel, *Superalloys II* (Wiley, New York, 1987; Metallurgiya, Moscow, 1995).
4. I. V. Doronin, I. N. Kidin, M. N. Kryanina, et al., "Anomalous Plastic Deformation in Nichrome," Izv. Vyssh. Uchebn. Zaved., Ser. Fiz., No. 11, 12–17 (1970).
5. S. T. Kishkin, A. I. Kovalev, and I. M. Khatsinskaya, "Short-Range Order in Heat-Resistant Nickel Alloys," in *S. T. Kishkin. Production, Study, and Application of Heat-Resistant Alloys: Selected Papers (to 100th Anniversary of Birthday)* (Nauka, Moscow, 2006), pp. 76–85 [in Russian].
6. A. Marucco, "Phase Transformations during Long-Term Ageing of Ni–Fe–Cr Alloys in the Temperature Range 450–600 C," Mater. Sci. Eng. **194** (2), 225–233 (1995).
7. I. N. Kidin, M. A. Shtremel', and A. P. Gruzdov, "Kinetics of Changes of Electrical Resistance in Ni–Cr Solid Solutions," Izv. Vyssh. Uchebn. Zaved., Chern. Metall. No. 11, 186–193 (1963).
8. B. M. Isakov, "On the Nature of the Anomalous Change of Electrical Resistance of Nichrome," Izv. Akad. Nauk Resp. Kazakhstan, Ser. Fiz. Mat. No. 6, 14–20 (1992).
9. E. Metcalfe, B. Nath, and A. Wickens, "Some Effects of the Ordering Transformation in Nimonic 80A on the Stress Relaxation Behavior," Mater. Sci. Eng. **67** (2), 157–162 (1984).
10. N. R. Dudova, R. O. Kaibyshev, and V. A. Valitov, "Manifestation of the Portevin–Le Chatelier Effect in the Kh20N80 Alloy," Fiz. Met. Metalloved. **105** (1), 105–112 (2008) [Phys. Met. Metallogr. **105** (1), 98–105 (2008)].
11. E. Lang, V. Lupinc, and A. Marucco, "Effect of Thermomechanical Treatments on Short-Range Ordering and Secondary-Phase Precipitation in Ni–Cr-Based Alloys," Mater. Sci. Eng., A **114**, 147–157 (1989).
12. I. N. Kidin, M. A. Shtremel', and V. Yu. Chizhikov, "Strengthening of Ni–Cr Solid Solution upon Tempering," Izv. Vyssh. Uchebn. Zaved., Chern. Metall. No. 5, 124–129 (1964).
13. R. Kaibyshev, N. Gajnutdinova, and V. Valitov, "Deformation Behavior of a Commercial Ni–20% Cr Alloy," in *Creep and Fracture of Engineering Materials and Structures*, Ed. by J. D. Parker (Institute of Materials, London, 2001), pp. 417–425.
14. T. Kawabata, T. Kanai, and O. Izumi, "Positive Temperature Dependence of the Yield Stress in $TiAlL1_0$ Type Superlattice Intermetallic Compound Single Crystals at 293–1273 K," Acta Metall. **33** (7), 1355–1366 (1985).
15. A. Couret and D. Caillard, "Prismatic Slip in Beryllium. I. The Controlling Mechanism at the Peak Temperature," Philos. Mag. A **59** (4), 783–800 (1989).
16. A. Couret and D. Caillard, "Prismatic Slip in Beryllium. II. The Origin of the Strength Anomaly," Philos. Mag. A **59** (4), 801–819 (1989).
17. V. P. Kolotushkin, V. P. Kondrat'ev, A. V. Laushkin, and V. N. Rechitskii, "Effect of Long Aging on the Structure and Phase Stability and Properties of Ni–Cr Alloys," Metalloved. Term. Obrab. Met., No. 11, 7–10 (2003).
18. J. Bursik and M. Svoboda, "The Existence of P-Phase and Ni_2Cr Superstructure in Ni–Al–Cr–Mo System," Scr. Mater. **39** (8), 1107–1112 (1998).
19. A. Arya, G. K. Dey, V. K. Vasudevan, and S. Banerjee, "Effect of Chromium Addition on the Ordering Behavior of Ni–Mo Alloy: Experimental Results vs. Electronic Structure Calculations," Acta Mater. **50**, 3301–3315 (2002).
20. O. Sitdikov and R. Kaibyshev, "Dislocation Glide and Dynamic Recrystallization in LiF Single Crystals," Mater. Sci. Eng., A **328** (1–2), 147–155 (2002).
21. R. Kaibyshev, O. Sitdikov, I. Mazurina, and D. R. Lesuer, "Deformation Behavior of a 2219 Al Alloy," Mater. Sci. Eng., A **334**, 104–113 (2002).
22. K. S. Ghosh, K. Das and U. K. Chatterjee, "Kinetics of Solid-State Reactions in Al—Li–Cu–Mg–Zr Alloys from Calorimetric Studies," Metall. Mater. Trans. A, **38**, 1965–1975 (2007).
23. S. Muneki, H. Okada, H. Okubo, et al., "Creep Characteristics in Carbon Free New Martensitic Alloys," Mater. Sci. Eng., A **406**, 43–49 (2005).
24. M. A. Shtremel' and F. F. Satdarova, "Effect of "Vacancy Quenching" on Changes in Short-Range Order," Fiz. Met. Metalloved. **30** (1), 10–15 (1970).
25. R. Kaibyshev and I. Kazakulov, "Deformation Behavior of Fe–3% Si Steel," Mater. Sci. Techn. **20** (2), 221–228 (2004).
26. D. Haussler, M. D. Bartsch, U. Messerschmidt, and B. Reppich, "HVTEM in situ Observations of Dislocation Motion in the Oxide Dispersion Strengthened Superalloy MA 754," Acta Mater. **49** (18), 3647–3657 (2001).
27. R. Kaibyshev, F. Musin, E. Avtokratova, and Y. Motohashi, "Deformation Behavior of a Modified 5083 Aluminum Alloy," Mater. Sci. Eng., A **392** (1–2), 373–379 (2005).
28. B. Bay, N. Hansen, D. A. Hughes, and D. Kuhlmann-Wilsdorf, "Evolution of FCC Deformation Structures in Polyslip," Acta Mater. **40**, 205–219 (1992).
29. V. V. Rybin, *Large Plastic Deformations and Fracture of Metals* (Metallurgiya, Moscow, 1986) [in Russian].